JOURNAL OF PROPULSION AND POWER
Vol. 9, No. 2, March–April 1993

Wake Mixing and Performance of a Compressor Cascade with Crenulated Trailing Edges

S. J. DeCook,* P. I. King,† and W. C. Elrod‡
Air Force Institute of Technology, Wright-Patterson Air Force Base, Ohio 45433

Trailing-edge crenulations have been shown to enhance velocity recovery (wake dissipation) and to decrease total pressure losses in the blade wakes downstream of a low-aspect ratio linear compressor cascade. A new study was performed to determine the influence of trailing-edge crenulations on outlet flow in the presence of varied inlet flow conditions. Two levels of inlet flow turbulence intensity (about 0.15 and 3%) were combined with sidewall boundary-layer removal at the cascade inlet (on or off) to provide four test conditions. Results from blades with large and small crenulations were compared with unmodified blades. For each test condition, a reduction of 10–20% in both velocity variance (enhanced wake mixing) and total pressure loss was observed in the outlet flow with the crenulated blades, while a slight decrease in turning angle was also observed.

Nomenclature

C_p = cascade static pressure coefficient; blade
C_{p0} = cascade pressure coefficient for the solid blade
c = chord, mm
dy = increment in span direction
dz = increment in pitch direction
P_s = blade surface static pressure, bar
P_1 = inlet static pressure, bar
P_2 = outlet static pressure, bar
P_{01} = inlet total pressure, bar
P_{02} = outlet total pressure, bar
S = surface distance on blade, mm
S_0 = suction surface length, mm
s = blade spacing, mm
V_{x2} = outlet axial velocity, m/s
V_1 = inlet velocity, m/s
V_2 = outlet velocity, m/s
$\overline{V_2}$ = average outlet velocity, m/s
x = axial distance downstream of cascade, mm
z = span dimension encompassing measurements, mm
α_2 = gas outlet angle, deg
ρ_1 = inlet density, kg/m^3
ρ_2 = outlet density, kg/m^3
σ^2 = variance
$\bar{\omega}$ = total pressure loss coefficient
$\overline{\omega_0}$ = total pressure loss coefficient for the solid blade

Introduction

IN axial-flow compressor stages, the nonuniform velocities caused by blade wakes degrade the efficiency of downstream blade rows. In gas turbines, the downstream blade wakes inhibit efficient fuel and air mixing in the combustor and reduce combustion efficiency. In both cases, a reduction in the size of the wakes or a mixing out of the wakes would be beneficial. Wennerstrom[1] suggested that crenulated trailing edges on stator airfoils would break up and help mix out blade wakes. Crenulations, shown in Fig. 1, are small notches intended to generate counter-rotating vortices due to the pressure difference between the suction and pressure surfaces of the airfoil. At the time of Wennerstrom's patent, it was unclear to what extent crenulations would improve wake dissipation, and whether passage or stage performance would be degraded. Subsequently, Veesart et al.[2] found that in a subsonic compressor cascade (inlet Mach number $\approx$ 0.4) with low freestream turbulence, both large and small crenulations not only enhanced wake dissipation, but also decreased total pressure loss. The present authors felt that further studies with higher freestream turbulence merited study, since possibly the success of low turbulence results was due in part to an interaction of the crenulation vortices with the sidewall corner vortices which a higher freestream turbulence would tend to diffuse. It was also felt that the effects of sidewall suction at the cascade inlet needed further clarification since flow through a simulated high-aspect ratio cascade (suction on) would also reduce interactions between the crenulation vortices and sidewall corner vortices. Finally, the influence of the crenulations on static pressure rise through the cascade, needed quantification.

Freestream turbulence intensity and sidewall boundary layers influence the development of corner vortices which affect cascade performance, especially for low-aspect ratio cascades. In Fig. 2, surface oil movement shows the effects of sidewall and blade boundary-layer flow in the cascade for the unmodified blade. (Results for crenulated blades are identical). As the flow is turned through the passage, air in the sidewall boundary layers moves onto the blade suction surfaces (just past the half-chord point) and forms corner vortices with axes aligned approximately in the flow direction. The vortices are responsible for corner separation (stall), and as seen in regions where oil has not flowed, approximately 15% of the blade sees separated flow at a negative incidence of 1.6 deg (cf. Fig. 2b). The spanwise extent of these vortices is reduced with the addition of freestream turbulence or the application of upstream boundary-layer suction as shown in Figs. 2a, 2b, and 2d. Later, it is shown that total pressure losses are associated with the corner vortices. Additionally, these vortices partially

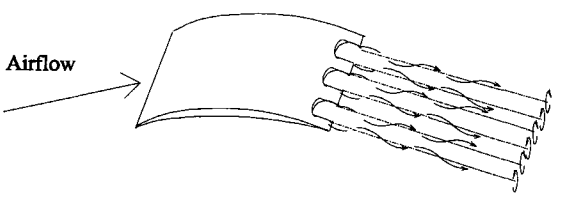

Fig. 1 Crenulated compressor blade.

Received May 5, 1992; revision received Nov. 3, 1992; accepted for publication Nov. 12, 1992. This paper is declared a work of the U.S. Government and is not subject to copyright protection in the United States.

*Graduate Student, Department of Aeronautics and Astronautics. Member AIAA.
†Associate Professor, Department of Aeronautics and Astronautics. Member AIAA.
‡Professor, Department of Aeronautics and Astronautics. Member AIAA.

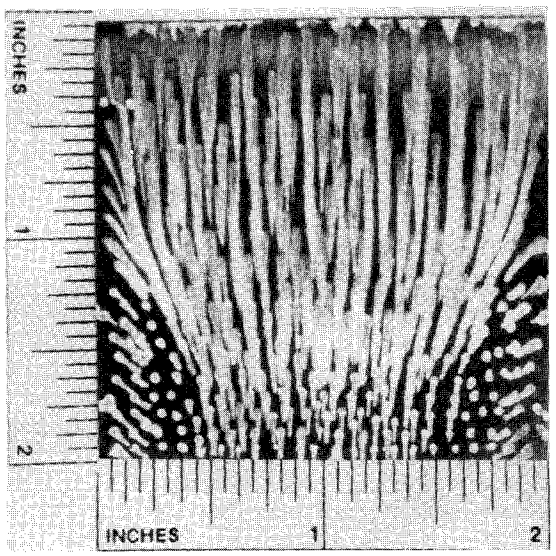

a) Suction on, turbulence off

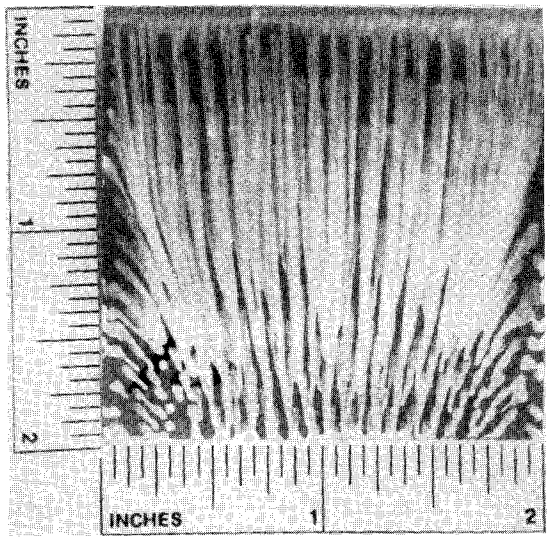

c) Suction on, turbulence on

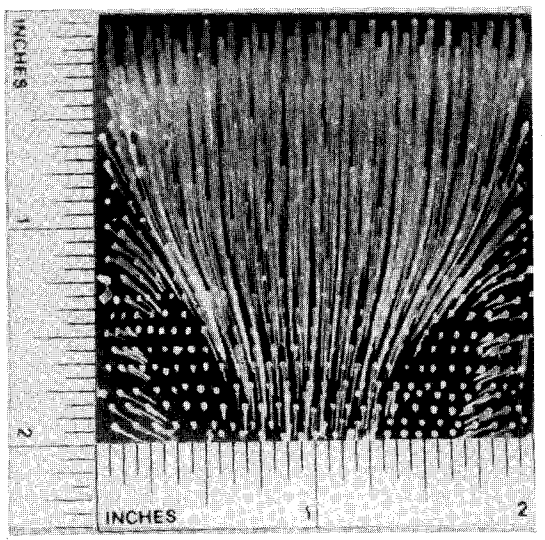

b) Suction off, turbulence off

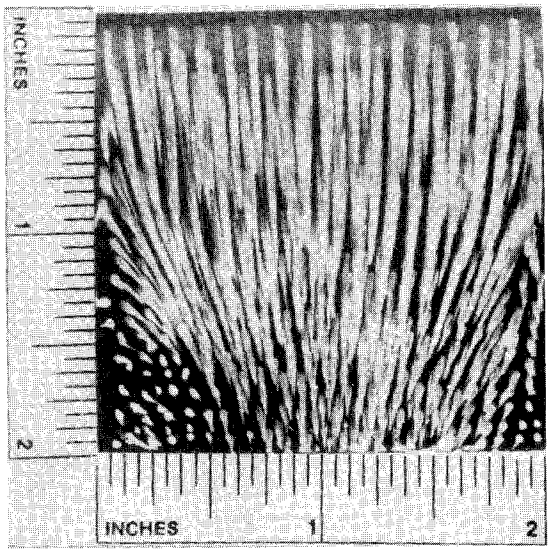

d) Suction off, turbulence on

Fig. 2 Suction surface boundary-layer flow patterns.

obstruct the passage and cause the flow along the centerline to be accelerated through the passage, degrading two-dimensionality. With suction on, the axial velocity density ratio (AVDR) for all blade configurations varied between 1.01–1.02, but removing the suction caused the AVDR to increase to about 1.045.

Although Lieblein[3] suggests that only turning angle and blade surface pressures are affected by non-two-dimensional flow, with pressure losses largely unaffected, the use of suction to improve AVDR markedly alters the extent of the corner vortices and can reduce total pressure losses for low-aspect ratio cascades.

Experimental work was performed on a low-aspect ratio, linear, compressor cascade. The upstream flow conditions were varied to examine the influence of two levels of freestream turbulence and sidewall boundary layer suction on the ability of trailing-edge crenulations to enhance wake mixing. Flows with low turbulence (0.15%) and moderate turbulence (3%), were generated by transverse jet air injection upstream of the cascade. Sidewall entering boundary layers were removed through a suction slot upstream of the cascade, which was either fully open or fully closed. The combination of two levels of freestream turbulence and two levels of suction produced four flow conditions identified as "suction on/off" and "turb on/off."

Experimental Apparatus and Procedures

Facility

The AFIT Cascade Test Facility is described by Veesart et al.[2] The test section includes a rectangular inlet duct, the cascade, and an outlet duct, each having a width (span) of 50.8 mm (2 in.). The cascade has seven blades arranged with a solidity (chord/space ratio) of 1.5, with two blades used as endwalls and the middle three exchanged for different crenulation configurations. The blades are NACA 64-A905 sections with 34.1 deg of camber, 50.8-mm (2.0-in.) chord, and 50.8-mm span. The blade stagger angle is 7.75 deg; the blade angles are 32.6 deg at the inlet and −1.5 deg at the outlet. With an inlet airflow angle of 31 deg, the flow incidence angle is −1.6 deg. The test section turns the flow about 30 deg and exhausts it through the outlet duct into the laboratory. This geometry approximates last-row stators in an axial flow compressor.

The cascade inlet stagnation pressure is constant at about 1.095 bar (1.4 psig), the static pressure upstream of the test section inlet about 0.966 bar (−0.5 psig), the mass flow about 1.45 kg/s (3.2 lbm/s), inlet velocity about 150 m/s (492 ft/s), outlet velocity about 131 m/s (430 ft/s), and inlet Reynolds number based on chord length of 415,000. A slot for sidewall boundary-layer removal parallel to the blade row is located

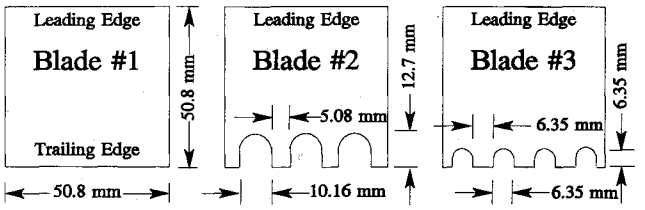

Fig. 3 Crenulation dimensions.

0.188-c lengths upstream of the blade row. The outlet duct is 317.5-mm (12.5-in.) long with tailboards adjusted for each blade configuration to eliminate any downstream pressure gradient in the suction-on, turbulence-off, flow condition.

Three 3-blade configurations using the middle three blades in the cascade were tested and are identified by blade type. As seen in Fig. 3, the configuration labeled blade 1 had an unmodified trailing edge, while that labeled blade 2 had three large crenulations in the trailing edge, and blade 3 had four small crenulations in the trailing edge. Measurements were made in the vicinity of the middle blade of the group which was also located centrally in the cascade.

Instrumentation

Instrumentation consisted of thermocouples, pressure transducers, pressure taps, a total pressure rake, and an x-hot film sensor. Two stepper motors positioned the hot film sensor or the pressure rake in the outlet flow, and two digitizers recorded the voltages. A Zenith Z-248 computer controlled the instrumentation, data acquisition, and reduction.

The inlet stagnation temperature and the ambient temperature were monitored by T-type thermocouples. Three static pressure taps, located about 2.4 chord lengths upstream of the middle blade of the cascade, were joined in a manifold to give the average inlet static pressure (upstream of the suction slot). The outlet duct had sidewall static ports, centrally located at 0.5-c increments downstream of the cascade, beginning at 0.25 c. The inlet stagnation pressure, ambient pressure, and cascade inlet and outlet static pressures were monitored by individual transducers which were accurate to about ± 0.00068 b (± 0.01 psi). In addition, 11 pressure transducers accurate to about ± 0.00020 b (± 0.003 psi) were used with a total pressure rake. Blade surface pressure taps were located as shown on a later figure for C_p values, and were staggered ± 0.8-mm off the centerline of the blade.

The total pressure rake, used for pressure loss and velocity data, has 11 equally spaced 0.7-mm outer diameter tubes spanning 38.1 mm (1.5 in.) or $\frac{3}{4}$ of the test section width. A Hewlett Packard 3455A digital voltmeter with 35-μV resolution at 24 samples/s, was used with an HP 3495 A Scanner to acquire pressure and temperature data. A ThermoSystems, Inc. (TSI) 1241-10 x-hot film probe was used with a TSI IFA100 anemometer and a TSI IFA200 digital voltmeter for turning angle and turbulence intensity measurements. The velocity measurements had a calculated accuracy of ± 0.8 m/s at 125 m/s (± 2.7 ft/s at 415 ft/s). Gas temperature changes were accounted for in the calibration procedure (DeCook[4]).

Turbulence Injection

Turbulence was introduced in the inlet duct through 16 air injection ports, 1.6-mm ($\frac{1}{16}$-in.) in diameter, located on the inlet duct perimeter about three chord lengths upstream of the middle blade of the cascade. Stagnation pressure was corrected for the effects of air injection upstream of the cascade test section. A loss of about 0.6% (0.0068 b or 0.1 psig) in stagnation pressure was consistently observed with the air injection on. No losses were observed in the flow without air injection.

With no air injection, a uniform turbulence intensity of about 0.15% was measured at the cascade inlet. With injection on, the turbulence intensity varied from about 3.5% near the top of the cascade to about 2.5% near the bottom of the cascade, yielding 3% at the measurement passages (middle three blades). Gostelow[5] suggests that any increase in turbulence above a low, quiescent value has the strongest effect on performance and losses, whereas, further increases have less of an effect, and possibly little or no effect. Roudebush[6] also suggests that freestream turbulence greater than 0.2% has a strong influence on the location of boundary-layer transition which directly affects the performance and losses of an airfoil.

Performance Measurements

Cascade performance is related to the changes in flow direction, static pressure rise through the cascade, and total pressure loss. The overall cascade pressure rise is represented by the static pressure coefficient $C_p = (P_2 - P_1)/(0.5\rho_1 V_1^2)$.

The loss in total (stagnation) pressure through the cascade was nondimensionalized by the inlet dynamic pressure to form the loss coefficient $\bar{\omega} = (P_{01} - P_{02})/(0.5\rho_1 V_1^2)$, where P_{02} is the mass-averaged value downstream. Data for mass averaging was collected with the total pressure rake in several planes parallel to the exit plane behind the cascade (0.25, 0.5, 0.75, 1, 1.25, 1.75, 2.25, 3, and 4 c, respectively). At each measurement plane, the 11-tube rake was traversed $\pm\frac{1}{2}$ pitch above and below the center of the wake of the middle blade in the three-blade configuration in increments of 0.25 mm. (This yielded a matrix of values 11 $\times$ 134.) For each point in the matrix, velocity was calculated from one-dimensional compressible flow theory using the duct static pressure (wall values were assumed equal to stream values since the duct was narrow and the flow had no side skew), total pressure, and total temperature. The data were mass-averaged according to

$$\bar{A} = \frac{\int_{-s/2}^{s/2}\int_{-z}^{z} A\rho_2 V_{x_2}\, dz\, dy}{\int_{-s/2}^{s/2}\int_{-z}^{z} \rho_2 V_{x_2}\, dz\, dy} \tag{1}$$

where A is the quantity being mass averaged.

For C_p and $\bar{\omega}$, P_1 was measured upstream of the suction slot and its value varied with suction. Thus, suction-on and suction-off conditions are not directly comparable.

Wake dissipation (mixing) in the outlet flow was evaluated by the variance of velocities in the outlet flow at a given downstream location. Nondimensionalized by the mean outlet velocity, variance is defined by

$$\sigma^2 = \frac{1}{\overline{V_2}^2}\cdot\frac{\sum_{i=1}^{n}(V_{2_i} - \overline{V_2})^2}{(n-1)} \tag{2}$$

where n is the number of points sampled and the subscript i refers to individual points in the sample set.

α_2 was determined from data acquired with the x-hot film anemometer at one measurement station, 0.5-c downstream (similar measurements at several downstream locations showed little variation, with the overall average varying less than 0.15 deg from that at 0.5 c). At the 0.5-c station, measurements were made at five positions in the span direction, covering one crenulation space on each blade. Measurements in the pitch direction covered $\frac{1}{2}$ blade spacing above and below the center blade (68 points spaced at 0.5 mm). The results were mass-averaged according to Eq. (1) (the value of the angle in degrees replaced A).

Results and Discussion

Blade Surface Pressures

Each three-blade configuration had a center blade with suction surface pressure ports, whereas, only the solid blade (blade 1) had pressure surface pressure ports. Pressure coef-

ficients were calculated from $C_p = (P_s - P_1)/(0.5\rho_1 V_1^2)$, where P_s is the blade surface pressure and P_1 is the static pressure measured upstream of the suction slot.

A comparison of suction surface pressure coefficients are shown in Fig. 4. (The regions $S/S_0 \approx 0.25$ and $S/S_0 \approx 0.65$ did not contain pressure ports due to interference with the blade mounting pins). In Fig. 4, pressures for the different blades are nearly identical except near the leading edge where crenulations exert a small influence. Other flow conditions yielded similar results, i.e., overlapping C_p for the three-blade configurations (see DeCook[4]).

Passage Pressure Coefficient

The pressure coefficient for the unmodified (solid) blade with no suction and low turbulence was 0.206 (± 0.002 estimated accuracy). Uncertainties as to the effects of increased freestream turbulence and sidewall suction on inlet dynamic and static pressures made a universal comparison of pressure rise values unwarranted. However, the ratio of C_p for the crenulated blades to C_{p0} for the solid blade can be validly compared for a given flow condition. As shown in Fig. 5, the crenulations cause only minor reductions in C_p, although the large crenulations have a marginally lower pressure rise (note the scale). In two instances, C_p was slightly improved with the small crenulations. In each case the C_p for the crenulated blades were greater with increased secondary flow activity, i.e., no suction and high turbulence.

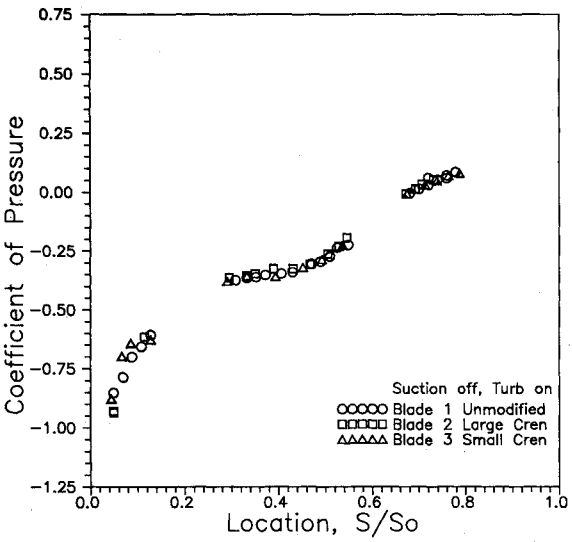

Fig. 4 Suction surface pressure coefficient.

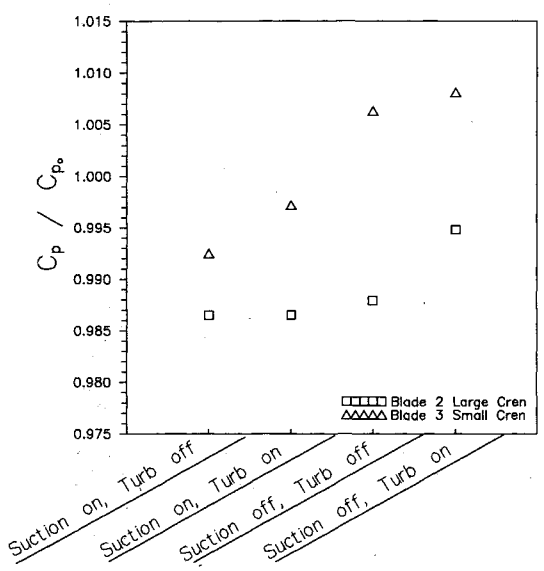

Fig. 5 Normalized static pressure rise across cascade.

Turning Angle

α_2 was measured with an x-hot film and mass-averaged according to Eq. (1), with an estimated accuracy of ± 0.35 deg. Measured values were between 1–2 deg for the exit gas angle (which yielded 0.317 for the diffusion factor for the unmodified blades with suction). Howell's criterion (Dixon[7]) predicts an outlet gas angle of 3.87 deg for a two-dimensional version of this configuration, which according to Cumpsty,[8] would lead to a diffusion factor of 0.294. It appears then that the low-aspect ratio blade combined with secondary flow effects (freestream turbulence, suction, sidewall vortices) increase the turning by 1–2 deg over values expected for a large aspect ratio blade. It should be noted that the span of measurements included only one full crenulation, and that near-wall flow would affect results if data were collected across the full span. Flow turning conditions ($31 - \alpha_2$) are presented in Fig. 6 for 0.5-c downstream. Note that captions are arranged differently from Fig. 5 to discriminate among the various flow effects. In general, the addition of higher turbulence reduced the turning angle by about 1 deg, while the addition of upstream sidewall suction increased the turning angle by roughly 0.5 deg (an average over five runs). Therefore, turning is decreased with the strengthening of either secondary flow effect, turbulence, or sidewall vortices. Interestingly, the effects of turbulence and suction appear to be uncoupled. The turning angles are slightly higher than predicted by correlations of two-dimensional cascade data, which indicate about 27.1 deg (Dixon[5]) or 27.9 deg (Lieblein[3]). As suggested by Erwin and Emery,[9] three-dimensional effects can cause this angle to be less or greater than two-dimensional results.

The large crenulations decreased the turning angle by an average of 0.85 deg, and the small crenulations decreased the turning angle by an average of 0.35 deg (five-run average), results which are most likely due to the missing trailing edge material in the crenulations. While the crenulations do not significantly influence turning, the small crenulations are slightly favored over the larger crenulations, as with the passage pressure rise results.

Total Pressure Loss Contours

Contours of total pressure loss coefficient at one chord length downstream, are shown in Figs. 7–9. In Fig. 7, the large areas of pressure loss near the sides are due to the corner vortices. (The large areas with no contours, near the top and bottom of the figure, are in the passage outside of the wake, and have almost no pressure loss.) In Fig. 7 it is seen that the losses are lowest with sidewall suction-on and low turbulence, particularly in the central region of the wake. An increase in the freestream turbulence thickens the wake and the extent of the corner vortices, spreading the losses over a larger area (resulting in a larger overall pressure loss). The most extensive

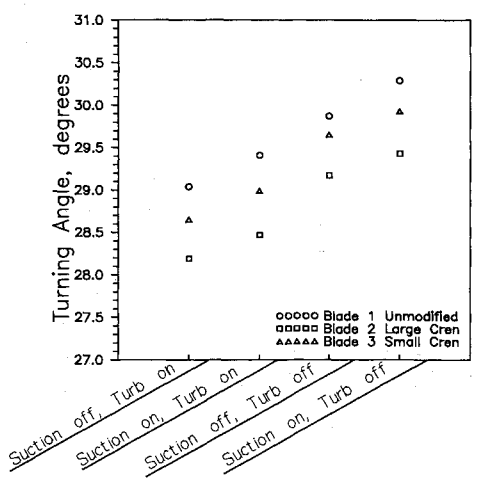

Fig. 6 Flow turning angle.

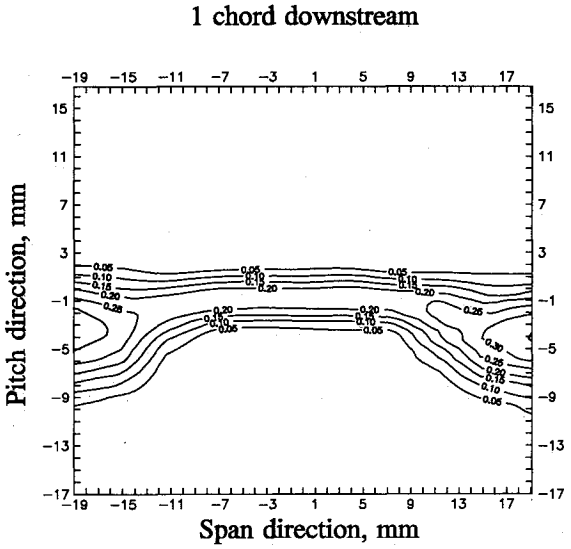

a) Suction on, Turb off Blade 1 Unmodified

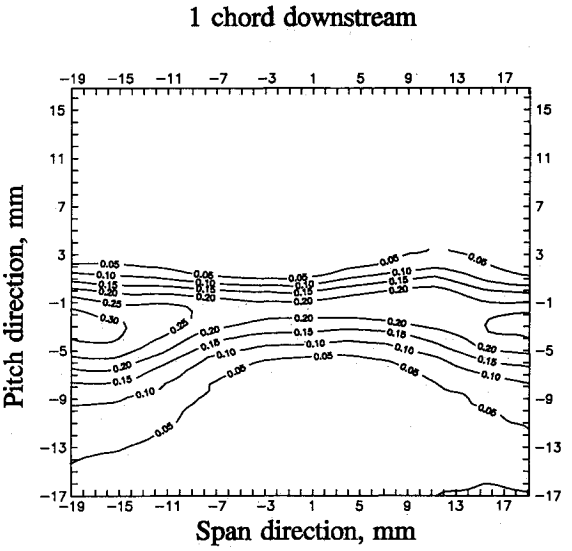

c) Suction on, Turb on Blade 1 Unmodified

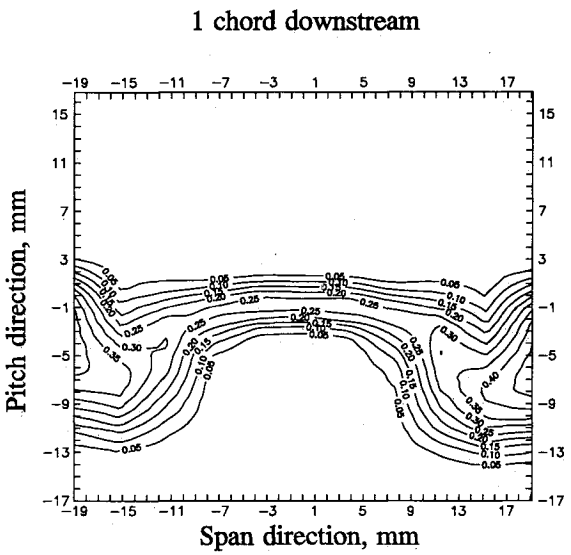

b) Suction off, Turb off Blade 1 Unmodified

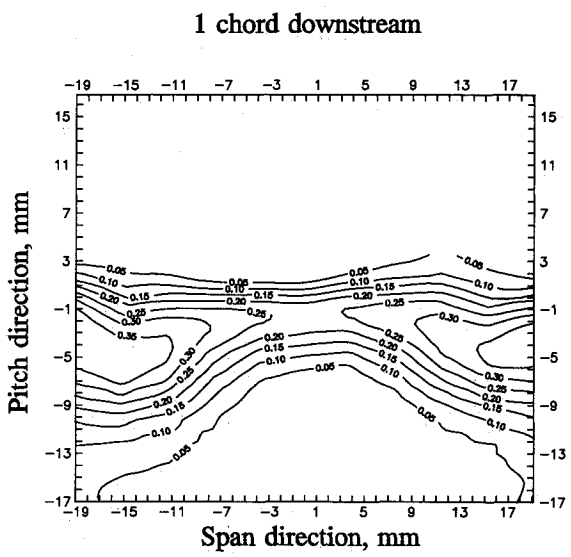

d) Suction off, Turb on Blade 1 Unmodified

Fig. 7 Pressure loss coefficient contours with unmodified blades.

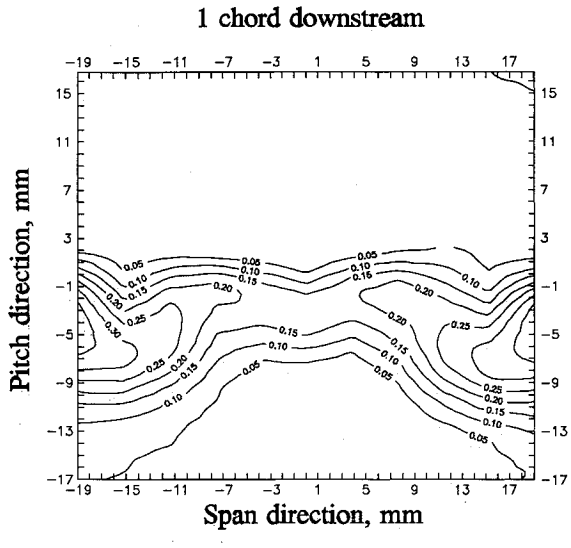

Suction off, Turb on Blade 2 Large Cren

Fig. 8 Pressure loss coefficient contours with large crenulations.

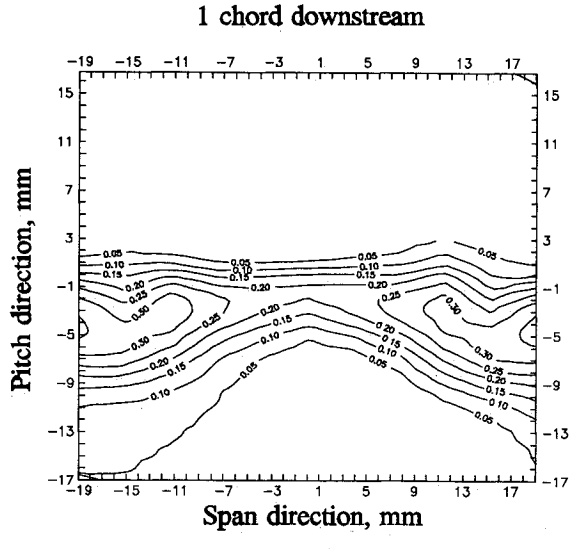

Suction off, Turb on Blade 3 Small Cren

Fig. 9 Pressure loss coefficient contours with small crenulations.

region of loss occurs for the suction-off, turbulence-on flow condition in Fig. 7d, i.e., the condition with highest activity of secondary flows. (The missing values in Figs. 7c and 7d at the 3-mm pitch location are due to faulty pressure readings.)

The influence of the crenulations on the outlet flowfield can be seen in Figs. 8 and 9, which show the results for the high-loss flow condition, suction-off, turbulence-on. To a larger degree, the large crenulations tend to diffuse the gradient of losses in the pitch direction while reducing the losses in the core of the wake (and to some extent reducing the losses in the corner vortex region). Both blades, however, exert a similar beneficial influence over the solid blade, as can be seen in a comparison with Fig. 7d. The influence of the crenulations on the outlet flow was similar for the other three flow conditions.

Total Pressure Losses

The total pressure losses for the suction-off condition are shown in Fig. 10. Total pressure losses are composed of losses through the cascade (from measurements made at the cascade outlet), wake mixing losses (which occur within the first half-chord length downstream from the cascade, according to Lieblein and Roudebush[10]), and outlet duct losses (which occur through further downstream mixing and incorporation of duct

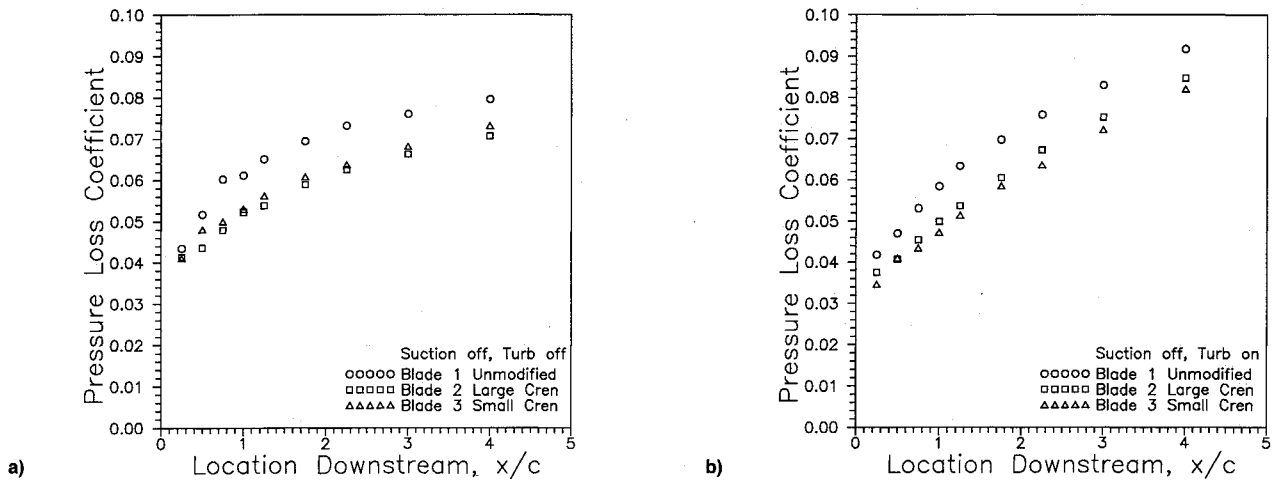

Fig. 10 Total pressure loss coefficient.

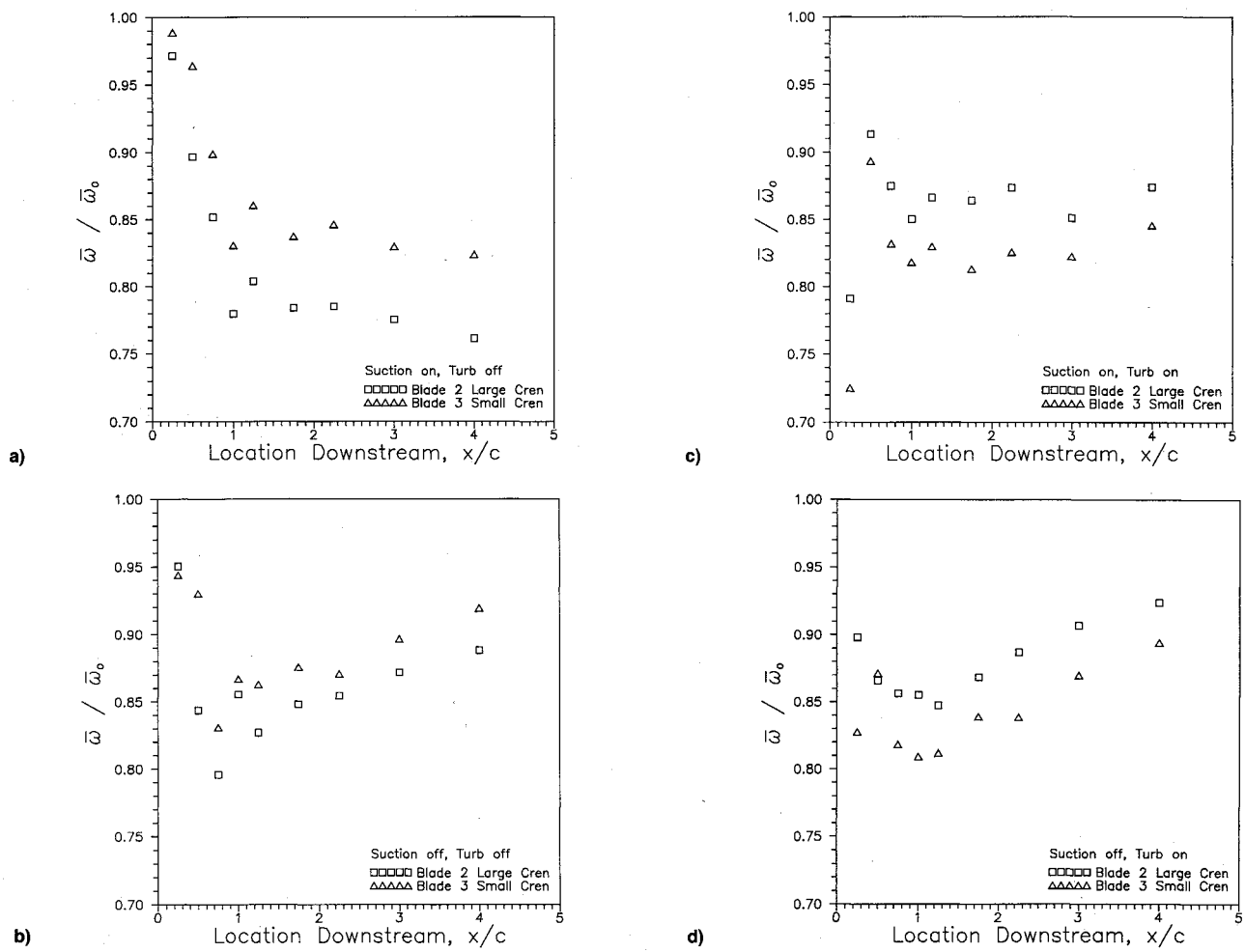

Fig. 11 Ratio of total pressure loss coefficients.

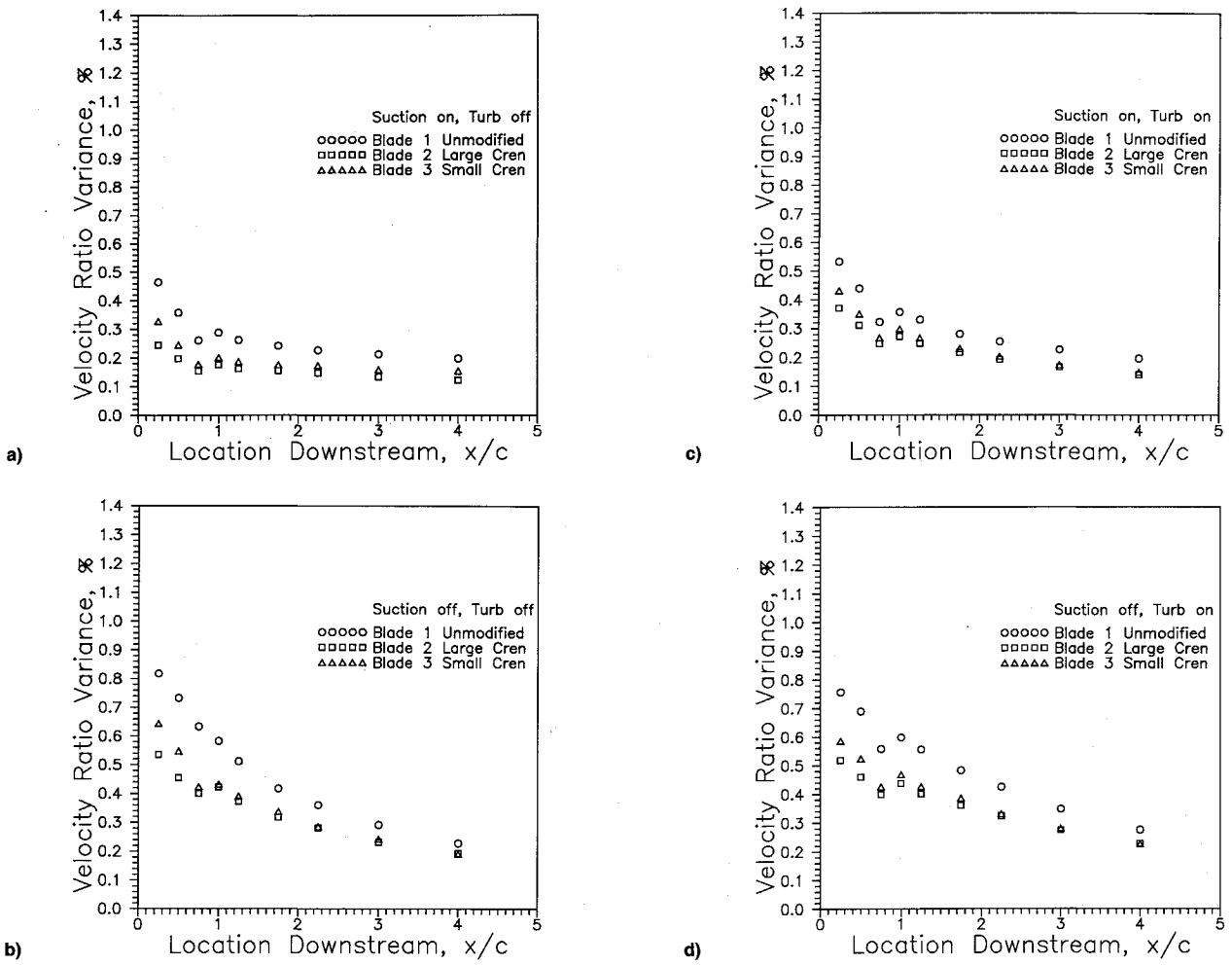

Fig. 12 Normalized outlet velocity variance.

sidewall boundary layers). Figure 10 shows that the crenulated blades cause lower pressure losses in all three regions (a new and unexpected result). Also in Fig. 10, it can be seen that in the higher turbulence flow, losses grow more rapidly with distance downstream, an indication that losses due to the outlet duct increase in turbulent flow. Similar trends, but with slightly lower values, occurred for the suction-on cases.

The effects of the crenulations are best seen in Fig. 11, which shows the ratio of the loss coefficient for the crenulated blades to that of the solid blade. In all flow cases there is a derived benefit with the crenulated blades. Although the total pressure loss increases with distance downstream (Fig. 10), the improvements with the crenulated blades remain roughly constant, an indication that the crenulations do not add to or decrease the losses induced by the walls of the outlet duct. Thus, the effect of the crenulations is mainly in the reduction of pressure losses associated with wake mixing. Figure 11 also shows that while the differences in losses between the two crenulation sizes are rather small, the large crenulations are more beneficial in low turbulence, suction-on (least secondary flow activity), and the small crenulations are best with higher turbulence, suction-off (highest secondary flow activity).

Wake Dissipation

Wake dissipation was characterized by the variance of outlet velocity normalized by the local mean velocity, and is presented in Fig. 12. As the flow moves downstream, the wakes decay and become mixed out, and the velocity variance eventually reduces to a constant value between 0.1–0.2% (the spanwise traverse included a portion of the duct wall boundary layer). It is to be noted that for any of the four flow conditions, the variance for the crenulated blades is lower than for the unmodified blades, particularly in the near-blade region, a proof of the concept promoted by Wennerstrom.[1] The crenulations seem to only slightly affect the rate of variance decay compared to the solid blade, suggesting that the distance for fully mixed flow is not changed very much. The reduction of variance is greatest in the near-blade region, where interstage aerodynamics would be most affected, and here the large crenulations do a better job of mixing the blade wakes. In the far region, differences between the two crenulation configurations are smaller, and for a very long mixing duct it is probable that improvements with crenulations would be minimal.

Conclusions

Reported in this study are the effects of crenulated trailing edges in the presence of varied secondary flow effects (freestream turbulence and sidewall vorticity) for a low-aspect ratio cascade. Both sizes of crenulations enhanced wake mixing with the new and unexpected result of reduction in total pressure losses. Enhanced mixing caused by the crenulations is not diminished, even in the presence of increased freestream turbulence and varied corner vortex strength. Turning angles were slightly reduced, and the pressure rise across the cascade was slightly reduced, except in two cases for the small crenulations. In general, the small crenulations caused the least degradation in turning angles and pressure rise, while the large crenulations caused slightly better mixing out of the wakes.

Further study is planned to include varied crenulation geometry and variations of Reynolds number, incidence angle, camber angle, and roughness.

Acknowledgments

The authors are indebted to Jay Anderson for support in the development of instrumentation for the experiment and Kevin Stanley for assistance in preparing the manuscript.

References

[1]Wennerstrom, A. J., "Vane Configuration for Fluid Wake Re-Energization," U.S. Patent 4,318,669, Washington, DC, 1982.

[2]Veesart, J. L., King P. I., Elrod, W. C., and Wennerstrom, A. J., "Wake Mixing Improvements in a Linear Compressor Cascade with Crenulated Trailing Edges," American Society for Mechanical Engineers Paper, 90-GT-218, Brussels, Belgium, June 1990.

[3]Lieblein, S., "Experimental Flow in Two-Dimensional Cascades," *Aerodynamic Design of Axial Flow Compressors (Revised)*, edited by I. A. Johnson and R. O. Bullock, NASA SP-36, Washington, DC, 1965.

[4]DeCook, S. J. *Experimental Investigation of Trailing Edge Crenulation Effects on Losses in a Compressor Cascade*, M.S. Thesis GAE/ENY/91D-1, School of Engineering, Air Force Inst. of Technology (AU), Wright-Patterson AFB, OH, Dec. 1991.

[5]Gostelow, J. P., *Cascade Aerodynamics*, Pergamon, New York, 1984.

[6]Roudebush, W. H., and Lieblein, S., "Viscous Flow in Two-Dimensional Cascades," *Aerodynamic Design of Axial Flow Compressors (Revised)*, edited by I. A. Johnson and R. O. Bullock, NASA SP-36, Washington, DC, 1965.

[7]Dixon, S. L., *Fluid Mechanics, Thermodynamics of Turbomachinery*, 3rd ed., Pergamon, New York, 1976.

[8]Cumpsty, N. A., *Compressor Aerodynamics*, Longman Group, Essex, England, UK, 1989.

[9]Erwin, J. R., and Emery, J. C., "Effect of Tunnel Configuration and Testing Technique on Cascade Performance," NACA TN-2028, 1950.

[10]Lieblein, S., and Roudebush, W. H., *Low Speed Wake Characteristics of Two-Dimensional Cascade and Isolated Airfoil Sections*, NACA TN-3771, Washington, DC, 1956.